"The **more** opportunities there are to get **students involved**, the more you will **encourage** previously unreached and **unrepresented groups** to join the Earth and Space science community."

Ryan Haupt
Research Fellow,
Smithsonian Museum
of Natural History
2015 Student Travel
Grant Recipient

Support the next generation of Earth and space scientists.
Donate to the Austin Student Travel Grant Challenge.

AGU100 ADVANCING EARTH AND SPACE SCIENCE

agu.org/austin | #AGU100

AGU PUBLICATIONS

Water Resources Research

RESEARCH ARTICLE
10.1002/2015WR017126

A new general 1-D vadose zone flow solution method

Fred L. Ogden[1], Wencong Lai[1], Robert C. Steinke[1], Jianting Zhu[1], Cary A. Talbot[2], and John L. Wilson[3]

[1]Department of Civil and Architectural Engineering, University of Wyoming, Laramie, Wyoming, USA, [2]Coastal and Hydraulics Laboratory, Engineer Research and Development Center, U.S. Army Corps of Engineers, Vicksburg, Mississippi, USA, [3]Department of Earth and Environmental Science, New Mexico Tech, Socorro, New Mexico, USA

Key Points:
- We have found a new solution of the general unsaturated zone flow problem
- The new solution is a set of ordinary differential equations
- Numerically simple method is guaranteed to converge and to conserve mass

Correspondence to:
F. L. Ogden,
fogden@uwyo.edu

Citation:
Ogden, F. L., W. Lai, R. C. Steinke, J. Zhu, C. A. Talbot, and J. L. Wilson (2015), A new general 1-D vadose zone flow solution method, *Water Resour. Res.*, *51*, 4282–4300, doi:10.1002/2015WR017126.

Received 19 FEB 2015
Accepted 22 APR 2015
Accepted article online 28 APR 2015
Published online 17 JUN 2015

Abstract We have developed an alternative to the one-dimensional partial differential equation (PDE) attributed to Richards (1931) that describes unsaturated porous media flow in homogeneous soil layers. Our solution is a set of three ordinary differential equations (ODEs) derived from unsaturated flux and mass conservation principles. We used a hodograph transformation, the Method of Lines, and a finite water-content discretization to produce ODEs that accurately simulate infiltration, falling slugs, and groundwater table dynamic effects on vadose zone fluxes. This formulation, which we refer to as "finite water-content", simulates sharp fronts and is guaranteed to conserve mass using a finite-volume solution. Our ODE solution method is explicitly integrable, does not require iterations and therefore has no convergence limits and is computationally efficient. The method accepts boundary fluxes including arbitrary precipitation, bare soil evaporation, and evapotranspiration. The method can simulate heterogeneous soils using layers. Results are presented in terms of fluxes and water content profiles. Comparing our method against analytical solutions, laboratory data, and the Hydrus-1D solver, we find that predictive performance of our finite water-content ODE method is comparable to or in some cases exceeds that of the solution of Richards' equation, with or without a shallow water table. The presented ODE method is transformative in that it offers accuracy comparable to the Richards (1931) PDE numerical solution, without the numerical complexity, in a form that is robust, continuous, and suitable for use in large watershed and land-atmosphere simulation models, including regional-scale models of coupled climate and hydrology.

1. Introduction

Appropriate treatment of the flow of water through unsaturated soils is extremely important for a large number of hydrological applications involving runoff generation such as: floods, droughts, irrigation, water quality, contaminant transport, residence time, ecohydrology, and the broad class of problems referred to as groundwater/surface water interactions. Our motivation to improve vadose zone modeling stability and algorithm efficiency is stimulated by the current development of high-resolution hydrologic models for the simulation of very large watersheds and similar efforts for regional-scale models of coupled climate and hydrology [*Ogden et al*. 2015a]. Such models require an accurate, efficient, and robust solution method coupling the land surface to groundwater and surface water to groundwater through the vadose zone that is guaranteed to converge and conserve mass.

Richards [1931] developed the fundamental nonlinear 1-D partial differential equation (PDE) for unsaturated flow through porous media by calculating the divergence of the vertical 1-D flux considering the driving forces of gravity and capillarity, here written in the mixed form as:

$$\frac{\partial \theta}{\partial t} = \frac{\partial}{\partial z}\left(K(\theta)\frac{\partial \psi(\theta)}{\partial z} - K(\theta)\right), \tag{1}$$

where θ is the volumetric water content (L^3L^{-3}), t is time (T), z is the vertical coordinate (L) positive downward, $K(\theta)$ is unsaturated hydraulic conductivity (LT^{-1}), and $\psi(\theta)$ is capillary pressure (head) (L) relative to atmospheric pressure, which is negative for unsaturated soils. In equation (1), the space z and time t coordinates are independent variables, while θ and ψ are dependent variables. The dependent variables are related by a closure relationship, $\theta(\psi)$ the soil-water retention function. Richards' equation (RE) is an advection-diffusion equation, and equation (1) is often written in the form of a 1-D advection-diffusion equation that is solely a function of the water content:

$$\frac{\partial \theta}{\partial t} = \frac{\partial}{\partial z}\left(D(\theta)\frac{\partial \theta}{\partial z} - K(\theta)\right), \quad (2)$$

where $D(\theta)=K(\theta)(\partial\psi(\theta)/\partial\theta)$, which is called the soil-water diffusivity ($L^2\,T^{-1}$). The first term in parentheses in equation (2) represents diffusion by capillarity, while the second term in parentheses represents advection due to gravity. For completeness, the head form of RE is:

$$C(\psi)\frac{\partial \psi}{\partial t} - \frac{\partial}{\partial z}\left[K(\psi)\left(\frac{\partial \psi}{\partial z} - 1\right)\right] = 0, \quad (3)$$

where $C(\psi)=\partial\theta/\partial\psi$ is the specific moisture capacity (L^{-1}). The RE is often written in the head (ψ) form because it offers two advantages. First, the ψ form of RE can solve both unsaturated and saturated flow problems, particularly if compressibility effects are included in the storage term. Second, in heterogeneous soil the pressure head is a spatially continuous variable and water content is not, particularly at the interface between discontinuous soil layers. However, the head-based form of the RE must be forced to conserve mass using a technique such as flux updating, which cannot be used in saturated RE cells [*Kirkland et al*., 1992] and can lead to mass balance errors. The difficulty in solving equations (1), (2), or (3) comes from nonlinearity and the presence of both diffusion and advection. A general mass-conservative numerical solution methodology for the RE was not developed until *Celia et al*. [1990], and that method is not guaranteed to converge for all soil properties and water content distributions.

The complexities associated with the numerical solution of equations (1)–(3) are many, and were elucidated by *van Dam and Feddes* [2000] and *Vogel et al*. [2001], among others. Despite drawbacks, the numerical solution of *Richards'* [1931] equation remains the standard approach for the solution of a host of problems that depend on soil water movement. The computational expense and risk of nonconvergence of the numerical solution of *Richards'* [1931] equation are significant barriers to its use in high-resolution simulations of large watersheds or in regional climate-hydrology models where solving the RE at hundreds of thousands or millions of points is required. Given that the numerical solution of *Richards'* [1931] equation is not guaranteed to converge, there is a risk in large watershed simulations that a small percentage of RE solutions jeopardize the stability of the entire model simulation.

Infiltration fluxes are fundamentally determined by advection, not diffusion. At low water content, transport through a porous medium becomes limited by a lack of connectivity, as penicular water exists in stable isolates [*Morrow and Harris* 1965], which renders liquid-water diffusion impossible. In unsaturated soils in the presence of gravity, water infiltrating into a partially saturated porous medium flows faster through larger pores because they are the most efficient conductors [*Gilding* 1990]. Capillarity then acts to move this advected water from these larger pore spaces into smaller pore spaces at the same elevation in a process we call "capillary relaxation" after *Moebius et al*. [2012] who have observed this phenomenon using acoustic emissions.

This physical process of advection through larger pores with lower capillary suction and capillary relaxation into smaller pores with higher capillary suction produces sharp wetting fronts. Sharp fronts are common in infiltration, which can be problematic for the solution of equations (1) to (3). Regarding sharp fronts and their impact on general modeling of vadose zone processes, *Tocci et al*. [1997] wrote:

> Subsurface flow and transport solutions frequently contain sharp fronts in the dependent variable, such as fluid pressure or solute mass fractions, that vary in space and/or time; these fronts cause considerable computational expense. A good example of such a case is wetting-phase displacement of a nonwetting fluid in a uniform media, which results in a sharp fluid interface front that propagates through the domain for certain auxiliary conditions. Richards' equation (RE) is considered a state-of-the-art treatment for such a problem in an air-water system, although this formulation has been criticized as "paradoxical and overly simplistic." [*Gray and Hassanizadeh*, 1991]. RE is not only a good example of the broad class of problems of concern, but it is an equation with considerable intrinsic significance in the hydrology and soil science community; it will require improved solution schemes before practical problems of concern can be economically and accurately solved.

Numerical diffusion can create errors by smoothing sharp fronts in the numerical solution of equations (1)–(3) [*Ross*, 1990; *Zaidel and Russo*, 1992]. It follows, however, that improved solution methods are needed that can efficiently and accurately simulate unsaturated zone fluxes and sharp wetting fronts.

The approximate vadose zone flux solution method presented in this paper, which we refer to as the "finite water-content method," directly addresses this issue and follows from work published by *Talbot and Ogden* [2008], which we abbreviate as T-O. Their results agreed quite well with numerical solutions of RE in terms of calculated infiltration on multiple rainfall pulses. Since 2008, we have continued to improve the T-O method, testing it against analytical and numerical solutions of RE as well as laboratory data. In every test, the performance of the improved T-O methodology described in this paper was similar to the RE solution, and by some measures better, when compared against laboratory [*Ogden et al*. 2015b] data. This led us to hypothesize that the finite water-content method of *Talbot and Ogden* [2008] is actually an approximate general solution method of the unsaturated zone flow problem for infiltration, falling slugs, and vadose zone response to water table dynamics in an unsaturated porous medium that includes gravity and capillary gradients, but neglects soil water diffusivity, which is emphasized in *Richards'* [1931] equation [*Germann*, 2010]. In other words, compared to other infiltration laws and approximate solutions in the literature, our method is a general replacement for the RE for arbitrary forcing and water table conditions. Our method considers gravity and capillary head gradients in the case of infiltrating water and capillary water that is in contact with the water table, but neglects soil water diffusivity at the wetting front. This is addressed further in section 3.

Green and Ampt [1911] developed the first advection solution of the infiltration problem with uniform initial soil moisture. The *Green and Ampt* [1911] approximation was derived directly from the Richards equation by *Parlange et al*. [1982] who developed a three parameter infiltration method for nonponded surface boundary condition directly from a double integration of RE including both capillary and diffusion terms. *Parlange et al*. [1982] showed that both the *Green and Ampt* [1911] limit of a delta function diffusivity and the *Talsma and Parlange* [1972] limit of rapidly increasing D and $dK/d\theta$ could be obtained from their equation. The approach by *Parlange et al*. [1982] was extended to ponded infiltration by *Parlange et al*. [1985] and *Haverkamp et al* [1990], though in parametric form, which was later turned into an explicit formula by *Barry et al*. [1995], who showed how both the *Green and Ampt* [1911] solution and *Talsma and Parlange* [1972] solutions were simplified limits of their formulation. The infiltration formulation of *Parlange et al*. [1985] allows for arbitrary time-dependent surface ponding depth. *Smith et al*. [1993] added redistribution to the three-parameter infiltration model of *Parlange et al*. [1982]. *Chen et al*. [1994] developed a spatially averaged Green and Ampt approach to simulate infiltration in areally heterogeneous fields. *Parlange et al*. [1997] developed an approximate analytical technique to model infiltration with arbitrary surface boundary conditions. *Corradini et al*. [1997] improved on the method of *Smith et al*. [1993], with some simplification and testing over a range of soil parameters. *Triadis and Broadbridge* [2012] explored soil diffusivity limits, verified the infiltration equation of *Parlange et al*. [1982] and found that the wetting front potential is a function of time. None of the analytical infiltration solutions discussed in this paragraph considered a nonuniform initial soil water profile such as that created by a shallow water table, and while some of them are capable of simulating more than one rainfall event, none of them are what one would consider "continuous" models of infiltration.

Shallow water table conditions are very important to consider in hydrological modeling of large watersheds because these conditions affect rainfall partitioning, runoff generation, erosion, and flow path in riparian areas or areas of low-relief topography or in locations with shallow soils [*Loague and Freeze*, 1985; *Grayson et al*. 1992; *Downer and Ogden*, 2003, 2004; *Niedzialek and Ogden*, 2004]. *Salvucci and Entekhabi* [1995] developed an infiltration method that considered a nonuniform initial soil water profile with a homogeneous soil and a shallow, static water table. Their method assumed a piecewise linear infiltration front with variable capillary drive based on sorptivity theory. However, the method by *Salvucci and Entekhabi* [1995] is a single-event method. *Basha* [2000] developed multidimensional analytical expressions for steady state infiltration into a soil with a shallow water table. Neither of these two methods considered post infiltration redistribution or were capable of continuous simulations.

The primary difference between the prior work on analytical and approximate infiltration methods and the method discussed in this paper is that those approximations simulate infiltration, while the present method simulates not only infiltration, but the motion of surface-detached infiltrated water that is not in contact with the groundwater table, which we call "falling slugs," groundwater table motion effects, and redistribution and their subsequent effects on vadose zone soil water on a continuous basis. The wetting front model by *Clapp et al*. [1983] considered arbitrary soil water profiles, and is perhaps most similar to the method discussed in this paper, although there are numerous differences.

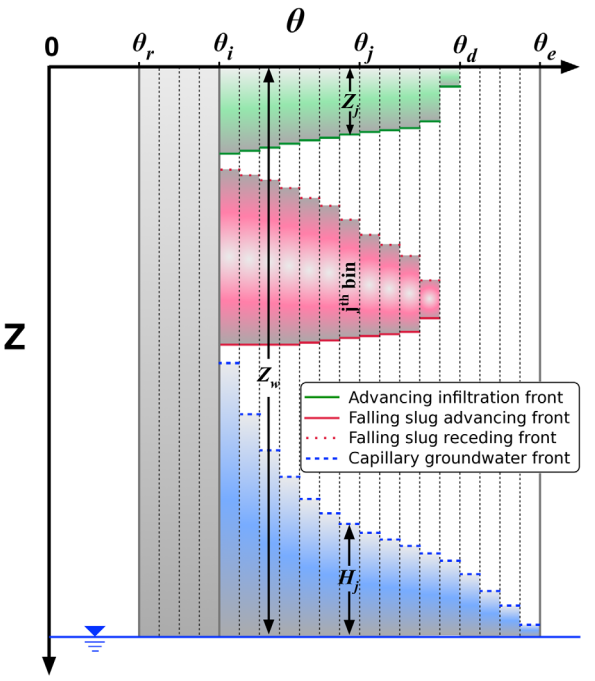

Figure 1. Finite water-content domain showing infiltration fronts (top, green), falling slugs (middle, red), and capillary groundwater fronts (bottom, blue) and capillary water that is in contact with both the water table and land surface (left, gray). The quantities z_j and H_j are positive as shown.

The method discussed in this paper builds and improves upon the finite water-content infiltration method developed by *Talbot and Ogden* [2008]. The developmental history that lead to *Talbot and Ogden* [2008] is as follows. *Ogden and Saghafian* [1997] derived a novel wetting front capillary drive function and followed the approach taken by *Smith et al.* [1993] to add redistribution to the *Green and Ampt* [1911] infiltration method. *Talbot and Ogden* [2008] extended the work of *Ogden and Saghafian* [1997] into the discretized water-content domain, and developed the two-step advance and capillary weighted redistribution procedure for simulating infiltration during multiple pulses of rainfall.

2. Finite Water-Content Discretization

The finite water-content discretization of the vadose zone that we consider is shown in Figure 1. The discretization of the solution domain in terms of water content assumes that the soil is homogeneous so that the media properties are not a function of vertical coordinate z, although they are clearly a function of θ. This figure demonstrates how a homogeneous porous medium may be divided into N discrete segments of water content space, $\Delta\theta$, which we refer to as "bins," between the residual water content θ_r, and the water content at natural saturation, the effective porosity θ_e. These bins extend from the land surface (z=0) downward. The finite water-content domain should not be confused with the "bundle of capillary tubes" analogy [*Arya and Paris*, 1981; *Haverkamp and Parlange*, 1986]. Unlike the bundle of capillary tubes model, our finite water-content bins are each in intimate contact with all others at the same depth and are free to exchange water between them in a zero-dimensional process that produces no advection at or beyond the REV scale.

At a particular depth, the water content in a bin is binary—that is to say that at a given depth z, a bin is either completely full of water or completely empty. In general, it is not necessary to attribute a particular pore size to a given bin, although capillary head and wetting contact angle considerations would allow this. Also, it might be advantageous to use a variable bin size $\Delta\theta$, one that is related to the pore-size distribution of a media. Furthermore, different distributions of bin sizes might significantly reduce the number of bins without adversely affecting solution accuracy.

The finite water-content vadose zone domain can contain four different types of water. The first type we can an "infiltration front," which represents water within a bin that is in contact with the land-surface, but not in contact with groundwater at any depth. This water is shown in Figure 1 in green, and is fed by rainfall, snowmelt, and/or ponded surface water. The distance in a particular bin j from the land surface to the infiltration front is denoted with z_j. The second type of vadose zone water is a "falling slug," as shown in red on Figure 1. This water is falling at a rate determined by the incremental hydraulic conductivity of its particular bin, and represents water that once was an infiltration front that detached from the land surface when its advance was no longer satisfied by rainfall, snowmelt, or ponded surface water. The third type of vadose zone water is water held up by capillarity that is in contact with a groundwater table but not in contact with the land surface. This water is colored blue in Figure 1, and is under the control of the groundwater table that is a distance z_w below the land surface. The distance from the water table to the top of the current capillary rise in each bin is denoted H_j, which is measured positive upward from the water table. The fourth type of water we identify is water in bins that is in contact with the land surface and the groundwater table

or, extends downward to an indefinite depth as an initial condition—similar to the uniform well-drained initial condition that is required by the traditional *Green and Ampt* [1911] approach. This water to the left of the bin denoted as θ_i is shaded gray in Figure 1.

Talbot and Ogden [2008] assumed that an infiltration front has a single value of ψ because the capillary demands of all bins are satisfied first by advance then by redistribution except for the right-most bin (with lowest ψ) that contains water. This right-most bin cannot take water from any other bin to the right and therefore remains unsatisfied. For this reason at an infiltration front, ψ is single-valued. Furthermore, the infiltration front has a single value of hydraulic conductivity *K*, which is given by the difference between the hydraulic conductivity of the right-most bin that contains water $K(\theta_d)$, and the hydraulic conductivity of the right-most bin that is in contact with either the groundwater or a uniform initial condition $K(\theta_i)$. This *K* value represents the ability of gravity to take water into the soil at the land surface interface.

We have improved our understanding of the finite water-content vadose zone method since *Talbot and Ogden* [2008]. Specifically, we have made five improvements to the method:

1. The capillary-weighted redistribution employed in *T-O* [2008] moved water vertically in the profile and was incorrect because our intention in simulating this process is that it is a free-energy minimization process that involves changes in interfacial energy, not potential energy. In the improved method, we call this process *capillary relaxation* after *Moebius et al*. [2012], as it moves water from regions of low capillarity to high capillarity at the pore scale and at the same elevation, producing no advection at or beyond the REV scale.
2. *Talbot and Ogden* [2008] included the influence of a static near-surface water table in terms of its effect on groundwater/surface water interactions, but had not developed the equation to describe the effect of water table dynamics on the vadose zone water content distribution. We developed and verified this equation [*Ogden et al*., 2015b] using data from a column experiment that was patterned after the experiment by *Childs and Poulovassilis* [1962].
3. *Talbot and Ogden* [2008] did not include equations describing the dynamics of falling slugs during periods of rainfall hiatus. Falling slugs are considered in this improved method and discussed in this paper.
4. *Talbot and Ogden* [2008] incorrectly used bin-centered values of $K(\theta)$ and $\psi(\theta)$ which made the solution sensitive to the number of bins, even for large numbers of bins. We now evaluate these two parameters at the right edge of each bin (Figure 1), which leads to convergence with increasing bin number.
5. *Talbot and Ogden* [2008] derived their equation from unsaturated zone mass conservation and from dynamics similar to the approaches used by *Garner et al*. [1970], *Dagan and Bresler* [1983], *Morel-Seytoux et al*. [1984], *Milly* [1986], *Charbeneau and Asgian* [1991], *Smith et al*. [1993], and *Ogden and Saghafian* [1997]. In this paper, the fundamental equation of motion is derived from the same equations as the derivation of the *Richards* [1931] equation.

Taken together, these improvements represent a significant advancement by placing the entire concept of the finite water-content vadose zone flux calculation method on a stronger theoretical foundation, and includes the influences of groundwater table dynamics and the motion of infiltrated water during rainfall hiatus. Whereas *T-O* [2008] reported the method as an approximation for simulating only infiltration, this paper presents a more rigorous derivation based on first principles and extends the method to continuously simulate not only infiltration, but falling slugs and groundwater dynamic effects on vadose zone soil water. Our method is an entirely new class of approximate solution of the *Richards* [1931] equation that is continuous and capable of simulating the influence of a shallow water table on infiltration, recharge, and runoff fluxes with evapotranspiration. Our method is a replacement for the numerical solution of *Richards'* [1931] equation in homogeneous soil layers when the user is willing to neglect the effects of soil water diffusivity.

3. Derivation

Mass conservation of 1-D vertically flowing incompressible water in an unsaturated incompressible porous medium without internal sources or sinks is given by:

$$\frac{\partial \theta}{\partial t} + \frac{\partial q}{\partial z} = 0. \tag{4}$$

where the flux q (LT^{-1}) can be described using the unsaturated Buckingham-Darcy flux equation:

$$q = -K(\theta)\frac{\partial \psi(\theta)}{\partial z} + K(\theta) \quad = \quad -D(\theta)\frac{\partial \theta}{\partial z} + K(\theta), \tag{5}$$

Substitution here of equation (5) into equation (4) gives the 1-D *Richards'* [1931] partial differential equation in mixed form (equation (1)) or water content form (equation (2)). Our solution does not take that approach. Rather we use chain rule operations [*Philip*, 1957; *Wilson*, 1974, equation (3.40)] to perform a hodograph transformation of equation (4) into another convenient form for unsaturated flow problems in which θ and z change roles, with z becoming the dependent variable and θ the independent variable along with time t. The cyclic chain rule is used to transform the first term in equation (4):

$$\left(\frac{\partial \theta}{\partial t}\right)_z = -\frac{(\partial \theta / \partial z)_t}{(\partial t / \partial z)_\theta} = -\frac{(\partial z / \partial t)_\theta}{(\partial z / \partial \theta)_t}, \tag{6}$$

while the chain rule is used to describe the second term in equation (4):

$$\left(\frac{\partial q}{\partial z}\right)_t = \left(\frac{\partial q}{\partial \theta}\right)_t \left(\frac{\partial \theta}{\partial z}\right)_t. \tag{7}$$

Substitution of equations (6) and (7) into equation (4) and eliminating like terms yields:

$$\left(\frac{\partial z}{\partial t}\right)_\theta = \left(\frac{\partial q}{\partial \theta}\right)_t. \tag{8}$$

Note that it is possible to arrive at equation (8) by applying the chain rule to the convective acceleration term in the nonconservative linear soil water transport equation:

$$\frac{\partial \theta}{\partial t} + \frac{\partial q}{\partial \theta}\frac{\partial \theta}{\partial z} = \frac{\partial \theta}{\partial t} + u(\theta)\frac{\partial \theta}{\partial z} = 0, \tag{9}$$

where $u(\theta) = \partial z/\partial t = \partial q/\partial \theta$ is the characteristic velocity of a water content θ, [*Smith*, 1983].

Evaluation of this characteristic velocity or the identical term from equation (8) by differentiating equation (5) with respect to θ gives:

$$u(\theta) = \left(\frac{dz}{dt}\right)_\theta = \frac{\partial q}{\partial \theta} = \frac{\partial}{\partial \theta}\left[K(\theta)\left(1 - \frac{\partial \psi(\theta)}{\partial z}\right)\right] = \frac{\partial K(\theta)}{\partial \theta}\left(1 - \frac{\partial \psi(\theta)}{\partial z}\right) - K(\theta)\frac{\partial^2 \psi(\theta)}{\partial z \partial \theta}. \tag{10}$$

The cross partial-derivative that is the last term on the right-hand side of equation (10) deserves discussion. At hydrostatic equilibrium in the case of capillary water above a groundwater table, $\partial\psi / \partial z = 1$ and this term is zero because $\partial/\partial\theta\ (\partial\psi/\partial z) = 0$. In the case of a moving water table, equilibrium conditions ($\partial\psi / \partial z = 1$) are most closely sustained in the right-most bins where the conductivity is highest. However, the occurrence of this condition requires that the velocity of the water table V_w ($L\ T^{-1}$) be somewhat less than the saturated hydraulic conductivity K_s. *Ogden et al.* [2015b] demonstrated using experimental data that when the water table velocity was 0.92 K_s this cross partial-derivative term is negligible. In the case of finite water-content bins on the left where there are significant deviations from equilibrium conditions, this cross partial-derivative term is multiplied by a very small value of $K(\theta)$, which makes this term small. In the case of infiltration, the fundamental assumption of the *Talbot and Ogden* [2008] method that the wetting front capillary head ψ is single valued everywhere along the wetting front renders this cross partial-derivative term zero because ψ is not a function of z. The resulting fundamental 1-D flux equation is therefore the remaining portion of equation (10):

$$\left(\frac{dz}{dt}\right)_\theta = \frac{\partial K(\theta)}{\partial \theta}\left(1 - \frac{\partial \psi(\theta)}{\partial z}\right). \tag{11}$$

One path to the solution of equation (8) is to solve it for $q(\theta,t)$ and $z(\theta,t)$ by integration [*Wilson*, 1974]:

$$\int \frac{\partial q}{\partial \theta} d\theta \quad = \quad \int \frac{\partial z}{\partial t} d\theta \tag{12}$$

by inserting equation (11) on the right-hand side. Instead, we adopt a finite water-content discretization in θ and replace the integrals with summations:

$$\sum_{j=1}^{N}\left[\frac{\partial q}{\partial \theta}\right]_j \Delta\theta \quad = \quad \sum_{j=1}^{N}\left[\frac{\partial z}{\partial t}\right]_j \Delta\theta, \tag{13}$$

using our uniform finite water-content bins where N is the total number of bins and $j \leq N$ is the bin index. Summing from $j=1$ to N, we have the effective porosity at natural saturation:

$$\theta_e = \sum_{j=1}^{N} \Delta\theta = N\Delta\theta. \tag{14}$$

If instead we sum over only the increments j up to the last bin that contains water d at a given depth z then the total soil water at that depth is:

$$\theta(z) = \sum_{j=1}^{d} \Delta\theta = d\Delta\theta. \tag{15}$$

With this approach, the conservation equation for each bin j is:

$$\left[\frac{\partial q}{\partial \theta}\right]_j = \left[\frac{\partial z}{\partial t}\right]_j. \tag{16}$$

We then substitute the appropriate version of equation (11) on the right-hand side, which depends on whether we are simulating infiltration, falling slugs, or water table motion effects on vadose zone water content, resulting in one ODE to solve in time for each bin. If the nonlinearity is sufficiently simple the ODEs can be solved analytically; in general, we use a numerical forward Euler method in time.

The Method of Lines [*Liskovets*, 1965; *Hamdi et al*. 2007] (MoL) was used to convert a vertically discretized 1-D Richards' equation to a system of ODEs by *Lee et al*. [2005], and applied by *Fatichi et al*. [2012]. The following sections discuss our use of the MoL in the context of our θ-discretization to convert the partial derivatives in equation (11) into finite difference forms, resulting in a set of three ODEs. This new method is advective, driven by gravity and capillary gradients, and without an explicit representation of soil water diffusivity, which necessitates a separate capillary relaxation step as discussed in section 3.4.

3.1. Infiltration Fronts

In the case of infiltration, water advances through a front that spans water contents ranging from the right-most bin that is in contact with both the land surface and the groundwater table θ_i to the right-most bin containing water θ_d (Figure 1). In the context of the method of lines, the finite-difference form of the partial derivative term $\partial K(\theta)/\partial\theta$ in equation (11) becomes:

$$\frac{\partial K(\theta)}{\partial \theta} = \frac{K(\theta_d) - K(\theta_i)}{\theta_d - \theta_i}. \tag{17}$$

Note that the quantity in equation (17) is the average velocity of the wetting front in the pore space between θ_i and θ_d neglecting capillarity [*Smith*, 1983; *Niswonger and Prudic*, 2004]. In the 1-D flux term from equation (11), the quantity 1-$\partial\psi(\theta)/\partial z$ represents the hydraulic gradient within the context of unsaturated Buckingham-Darcy flux. In the finite water content discretization within bin j, using the single-valued Green and Ampt wetting front capillary suction assumption as a reasonable first approximation, this term is replaced with $1+\frac{G_{eff}+h_p}{z_j}$, where G_{eff} is the wetting front effective capillary drive (positive) and h_p is the depth (L) of ponded water on the surface in the case of infiltration. The wetting front effective capillary drive G_{eff} is the greater of $|\psi(\theta_d)|$ or the value calculated as described by *Morel-Seytoux et al*. [1996, equations (13) and (15)] (L). These two changes inserted into the finite water-content discretization of equation (11) yields an ordinary differential equation describing the advance of vadose zone infiltration fronts in bin j:

$$\frac{dz_j}{dt} = \frac{K(\theta_d) - K(\theta_i)}{\theta_d - \theta_i}\left(1 + \frac{G_{eff} + h_p}{z_j}\right). \tag{18}$$

Equation (18) is identical to equation (6) from *Talbot and Ogden* [2008] with the exception of the subtraction of $K(\theta_i)$ from $K(\theta_d)$. The justification for the use of a single value of G_{eff} and $K(\theta_d)$ is provided in *Talbot and Ogden* [2008]. It is also important to note that in the limit as $t \to \infty$ with a constant applied flux that is less

than the saturated hydraulic conductivity (K_s) in an infinitely deep, well-drained soil with a uniform initial water content θ_i, $z_j \rightarrow \infty$ and the rate of advance in each bin is given by the finite difference approximation of the leading partial derivative $\partial K(\theta)/\partial\theta$.

In the case of a single bin in a deep well-drained homogeneous soil with uniform initial water content θ_i, equation (18) becomes the *Green and Ampt* [1911] equation, with $G_{eff} = H_c$, $\theta_d = \theta_e$, $K(\theta_i) = 0$, and $K(\theta_d) = K_{G\&A}$, $z_j = F/\Delta\theta$, with H_c and $K_{G\&A}$ representing the *Green and Ampt* [1911] capillary drive and hydraulic conductivity parameters, respectively, and F is the cumulative infiltrated depth. The *Green and Ampt* [1911] equation is a special case of the finite water-content method with only one constant $\Delta\theta$ bin and uniform initial water content.

Given a rate of rainfall or snowmelt in equation (18) for each infiltrating bin in the finite water-content domain, z_j and h_p are independent variables. Bin-specific values of $K(\theta)$ and $\psi(\theta)$ are constant and computed once for each bin using the water content associated with the right edge of each bin, which minimizes floating-point mathematical computations of the highly nonlinear $K(\theta)$ and $\psi(\theta)$ functions.

In the case of infiltration, the number of bins required to accurately describe the infiltration front profile is from between 150 and 200 between θ_r and θ_e. However, the number of bins can be reduced if the minimum water content expected in a simulation is greater than θ_r. All water to the left of θ_i can be combined into one bin that provides a flux to groundwater at the rate given by θ_i [*Smith et al.* 1993].

Because of the monotonically increasing nature of the $K(\theta)$ relation, and the fact that bins fill from left to right, which often results in decreasing z_j in bins to the right and hence larger dz/dt by equation (18), infiltration fronts in bins to the right of the profile can out-run infiltration fronts in bins to the left. This is a natural consequence of the physics where larger pore spaces are more efficient conductors of infiltrating water [*Gilding*, 1991] and that results in an overhanging profile or "shock" [*Smith*, 1983] as shown in Figure 2a, and results in the need for simulating capillary relaxation as discussed in section 3.4.

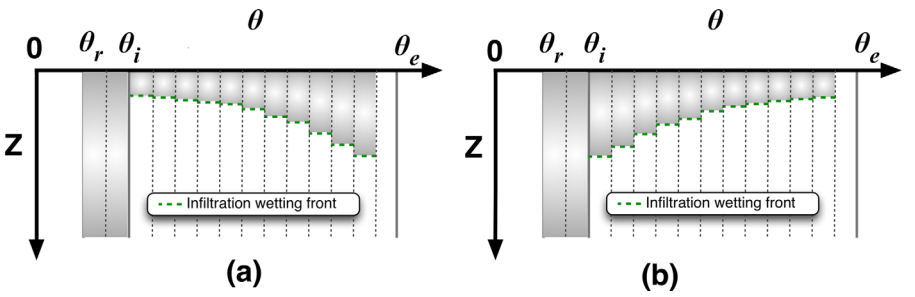

Figure 2. Water content profile (a) after infiltration step and (b) after capillary relaxation step. Exaggerated to illustrate the process. Note that there is no advection of water in the profile through this process.

3.2. Rainfall or Snowmelt Hiatus: Falling Slugs

During periods of time when the rainfall or snowmelt rates and/or surface ponding are insufficient to provide for the calculated advance of infiltrated water in bins using equation (18), "falling slugs" are created, as shown in Figure 1. With reference to equation (11), the capillary gradient $\partial\psi(\theta)/\partial z \approx 0$ and gravity is the only significant driving force. In this case, the water in those bins detaches from the land surface and "falls" through the medium at a rate calculated as the incremental hydraulic conductivity component associated with the value of θ_j for that bin [*Wilson*, 1974, equation (6.69)]:

$$\frac{dz_j}{dt} = \frac{K(\theta_j) - K(\theta_{j-1})}{\Delta\theta}. \tag{19}$$

Note that in applying equation (19) we have assumed that the dynamic wetting contact angle at both the top and bottom of this falling slug of water are the same, which means that the capillary forces are balanced and gravity is the only driving force. This results in the same velocities of the top and bottom ends of the slug. This assumption is not necessary and dynamic wetting contact angle effects could be included [*Hilpert*, 2010].

A falling slug in a bin will advance until it comes in contact with groundwater fronts deeper in the soil profile or until they disappear by capillary relaxation at the slug front. Because of the monotonically increasing

nature of the $K(\theta)$ relation, falling slugs in bins to the right of the profile will advance beyond falling slugs in bins to the left. This also results in the need for capillary relaxation as discussed in section 3.4.

3.3. Groundwater Table Dynamics Effects on Vadose Zone Water Content

In the case of a dynamic groundwater table, the water level in each bin will rise or fall relative to the difference between the top elevation of the water in a bin, which we call a "groundwater front," and the hydrostatic level for a given water table depth z_w. In the case of groundwater fronts, capillarity acts in the upward (-z) direction opposite gravity. With reference to Figure 1, water in the groundwater front ending in the jth bin can only travel through the pore space between θ_j and θ_i. In this case, the partial derivative term $\partial K(\theta)/\partial\theta$ in equation (11) is approximated by:

$$\frac{\partial K(\theta)}{\partial\theta} = \frac{K(\theta_j) - K(\theta_i)}{\theta_j - \theta_i}, \tag{20}$$

and equation (11) therefore becomes, together with the change of sign on the direction of capillarity and the fact that $dz = -dH$:

$$\frac{dH_j}{dt} = \frac{K(\theta_j) - K(\theta_i)}{\theta_j - \theta_i}\left(\frac{|\psi(\theta_j)|}{H_j} - 1\right), \tag{21}$$

where H_j is position of groundwater wetting front of bin j, defined as the distance from the top of the capillary rise down to the groundwater table. Note that in equation (21), when the capillary rise H_j is equal to the absolute value of the capillarity of the jth bin, $|\psi(\theta_j)|$, the water in this bin is in equilibrium and $dH_j/dt = 0$.

The groundwater wetting front dynamics can be affected by infiltration fluxes. Assuming a constant surface flux $f < K_s$ with a fixed water table, the hydrostatic groundwater front height above the water table can be approximated using [*Smith and Hebbert*, 1983]:

$$|\psi'(\theta_j)| = \frac{|\psi_b|}{1 - f/K_s} + \frac{|\psi(\theta_j)| - |\psi_b|}{1 - 0.5f/K(\theta_j) - 0.5f/K_s}, \tag{22}$$

where ψ_b is bubbling pressure head (L).

The behavior of equation (21) with capillarity modified as in equation (22) for applied flux effects was evaluated by *Ogden et al.* [2015b]. In that study, data from a column experiment fashioned after the water table dynamical tests of *Childs and Poulovassilis* [1962] were used to test equation (21) in the case of both falling and rising water tables. Equation (21) was also compared against the numerical solution of equation (3) using Hydrus-1D [*Simunek et al.* 2005]. The finite water-content vadose zone response to water table dynamics simulated using equations (21) and (22) compared favorably to Hydrus-1D. Compared against column observations, average absolute errors in predicted ponding times in the case of a rising water table were 0.29 and 0.37 h, for Hydrus-1D and the solution of equations (21) with (22), respectively. Ponding times predicted by both Hydrus-1D and the T-O method were more accurate for lower water table velocities. The finite water-content formulation had smaller RMSE and percent absolute bias errors in tests with a rising water table than the Hydrus-1D solution.

This method for simulating groundwater dynamics effects on vadose zone soil water offers a relatively simple method to include such effects in simpler infiltration schemes. For instance, *Lai et al.* [2015] found that only 10 groundwater bins allowed accurate simulation of the effects of water table dynamics on a Green and Ampt redistribution (GAR) scheme [*Ogden and Saghafian*, 1997].

In the case of groundwater front dynamics with a rapidly rising water table, groundwater fronts in bins to the right can out-pace groundwater fronts in bins to the left, resulting in an imbalanced profile. This results in the need to simulate capillary relaxation as described in section 3.4.

Coupling of this vadose zone solution to a two-dimensional groundwater model is a straightforward predictor-corrector scheme without iterations. The vadose zone solver behaves as a source or sink depending on the direction of groundwater table motion as determined by a saturated groundwater flow solver. The specific yield is calculated as a function of groundwater table depth [*Duke*, 1972; *Nachabe*, 2002]. If the

groundwater table falls in a time step, the T-O groundwater domain will give water to the groundwater table and cause it to fall at a slightly slower rate than what was originally calculated. In the case of a rising groundwater table, the opposite occurs, and the T-O vadose zone solver takes up water from the groundwater table, causing it to rise slightly less fast than originally calculated. Our solution of this problem is inherently stable and mass-conservative.

3.4. Capillary Relaxation

The finite water-content simulation approach is a two-step process, involving calculations of front or slug advance *dz/dt* in each bin followed by capillary relaxation. During infiltration calculated using equation (18), in the case of falling slugs using equation (19), or in the case of groundwater fronts using equation (21), higher velocities in bins to the right can result in an imbalanced profile as shown in Figure 2a. *Smith* [1983] called these shock fronts, and are analogous to kinematic shocks in kinematic wave flow theory [*Kibler and Woolhiser* 1972]. We posit that these shocks are dissipated by capillary relaxation [*Moebius et al.*, 2012], which involves movement of water *at the pore scale* from regions of lower capillarity to regions of higher capillarity. Capillary relaxation is a zero-dimensional internal process that produces no advection at or beyond the REV scale and does not change the dimensionality of our solution methodology. In the case of infiltration or groundwater fronts, this is equivalent to numerically sorting either the z_j or H_j values and putting them from maximum to minimum depth from left to right (higher ψ to lower ψ), as shown in Figure 2b. Falling slugs tend to decrease in water content as they propagate due to the effect of water in right-most bins passing water in bins to the left, and being pulled to the left by capillary relaxation. When implemented correctly, the process of capillary relaxation conserves mass perfectly by moving exact quantities of water between finite water-content bins using a finite-volume methodology.

3.5. Root Zone Water Uptake and Bare Soil Evaporation

Transpiration can remove water from bins in a specified root zone. For root water uptake, the potential transpiration demand is first calculated, then water within the root zone is removed from the right-most bin containing water, which has the lowest capillarity, until the demand is satisfied. This is consistent with the way plants remove water from the root zone [*Green and Clothier*, 1995]. Root water uptake can remove water from surface wetting fronts, falling slugs, and groundwater fronts if they are in the root zone. In the case of bare soil evaporation, a similar procedure can be used, with a specified top soil layer depth under primary evaporation influence (e.g., 5 cm). Secondary evaporation [*Or et al.* 2013] could be included, with potential evaporation able to remove surface ponded water.

3.6. Extension to Layered Soils

The finite water-content method was extended to simulate multilayer soils to consider soil heterogeneity. In each layer, the soil is assumed homogeneous. After each time step, the head is required to be single-valued at all layer interfaces. If the head in two adjacent layers differs, then water is moved upward or downward based on capillary demand or infiltration ability to restore single-valued head at the interface using the appropriate *dz/dt* equation.

Flow between layers is limited by the path-integrated hydraulic conductivity. In the infiltration process, if the upper layer is fully saturated, the water flow is limited by lower layer conductivity. For groundwater flow, if the lower layer is fully saturated, the upper layer flow is limited by the average conductivity of these two layers. The average hydraulic conductivity for M saturated layers of thickness D_p and saturated hydraulic conductivity $K_{s,p}$ is calculated using [*Ma et al.* 2010]:

$$\bar{K}_s = \frac{\sum_{p=1}^{M} D_p}{\sum_{p=1}^{M} D_p / K_{s,p}}. \tag{23}$$

Soil capillarity is determined by the $\psi(\theta)$ relation for the soil layer that contains the wetting front. The distance over which the capillary head gradient is calculated is the actual distance from the land surface to the wetting front in each bin, z_j in the case of infiltration, or $(z_w - H_j)$ in the case of groundwater fronts.

3.7. Conservation of Mass

Despite the fact that the derivation began with conservation of mass (equation (4)) there is nothing inherently mass conservative about equation (11) or its various forms (equations 18, 19, and 21). Conservation of mass is imposed upon the method by accurately accounting for all water added to and removed from the control volume using the finite-volume solution method.

Rainfall is added to the land-surface as the rainfall rate multiplied by the time step. At first, surface water is used to satisfy the demand of bins that are in contact with groundwater—the left-most gray-colored bins in Figure 1. That demand is given by $K(\theta_j)^*\Delta t$. Following that step, the advance Δz is calculated in bins that contain water using explicit forward Euler integration of equation (18). Those advancing bins take surface water until all those bins with water in them are satisfied or the surface water is gone. If surface water remains and new bins can take water, the initial advance Δz is limited by the maximum advance during a time step as described in *Talbot and Ogden* [2008]. In capillary relaxation of infiltration fronts, mass conservation is guaranteed by the fact that in this case, a simple sort is used that arranges the infiltration front from deepest to shallowest from left to right, with no net change in volume of water, as shown in Figure 2.

Falling slugs are first advanced using equation (19), which preserves their length. Falling slugs that encounter groundwater fronts during a time step are merged with the groundwater front, effectively raising the groundwater front nearer to the ground surface by an amount equal to the length of the merged slug in that bin. If the demands of the soil water bins that are in contact with groundwater (left-most gray bins in Figure 1) are not met, and there are no infiltration fronts, then that demand is satisfied from the right most falling slugs in the profile because this is the least tightly bound water in the soil. In a second step, capillary relaxation "clips" slug water to the right that is deeper than slugs to the left, and moves it as far as possible to the left in the profile. This process is inherently mass conservative when implemented correctly. Capillary relaxation at the leading edge of falling slugs invariably results in sharp fronts at the bottom of the slug.

In the case of groundwater fronts, advances or retreats are calculated using equation (21) with ψ values calculated from equation (22). If a constant head lower boundary condition is specified, then those advances or retreats are made for each bin taking from or giving water to the groundwater table. A capillary relaxation step is used to ensure that water rises monotonically from right to left in the profile. If the water table is allowed to vary, then a predictor-corrector step is used to better account for the effect of wetting front advances or retreats on changes in water table elevation in a way that is guaranteed to conserve mass.

One of the strengths of the finite-volume solution approach is that water can be added to or removed from the simulation domain at any point and at any time. This allows coupling with entities and/or processes that can act like sources and or sinks, such as macropores, soil pipes, roots, irrigation emitters, or drains.

3.8. Numerical Integration and Analytical Solutions

Generally, equations (18), (19), and (21) can be explicitly integrated using a forward Euler technique. Typical time steps vary by process. Preliminary analysis suggests that equation (18) requires a time step on the order of 10 s for simple forward Euler integration. *Yu et al*. [2012] demonstrated that the infiltration equation is guaranteed to converge and that the use of fourth-order Runge-Kutta integration allows longer time steps O(60 s). Preliminary analysis also suggests that falling slugs (equation (19)) require a time step on the order of 100 s, and groundwater fronts (equation (21)) can use a time step of up to 500 s. Under continuously ponded conditions, if the ponded depth h_p does not change with time, then equation (18) can be integrated directly to have an expression for z_j for any time t. The solution need not be expressed as explicitly as $z_j = f(t)$, rather it could be $f(z_j, t) = 0$. Newton-Raphson or another method will allow solution of $z_j = z_j(t)$ for any time. In some cases, the derived ODE does not require finite-differencing to solve.

Because of the finite-water content discretization, analytical solutions are possible using the MoL in several unique initial and boundary conditions. The first would be constant head ponding conditions from $t=0$, which would lead to a *Green and Ampt* [1911] solution. The second would be constant water table velocity from time $t=0$.

4. Test Results

4.1. Steady State Analytical Comparison of Multilayer Infiltration

Rockhold et al. [1997] developed an analytical solution technique using numerical integration for 1-D steady water flow in layered soils with arbitrary hydraulic properties. Following *Rockhold et al.* [1997], we performed a comparison of the finite water-content method in predicting steady state infiltration and soil water profiles in a 6 m deep soil column. This column contained three layers, each 2 m in thickness. The first and third layers were assumed to be a fine sand. The second layer consisted of a silty clay loam. The hydraulic properties of those soils using the van Genuchten model [*van Genuchten*, 1980] are given in Table 1 [after *Rockhold et al.*, 1997]. In the simulation, a fixed water table was specified at the lower boundary, and a constant flux of 1.6×10^{-4} cm/s was specified at the upper boundary.

Table 1. Soil Layer Properties for Three-Layer Steady Infiltration Test [After *Rockhold et al.*, 1997]

Texture	K_s (cm h^{-1})	α (cm^{-1})	n	θ_r	θ_s
Loamy fine sand	22.54	0.0280	2.2390	0.0286	0.3658
Silty clay loam	0.547	0.0104	1.3954	0.1060	0.4686

The steady state water content profiles from the finite water-content (T-O) method and Hydrus-1D are shown in Figure 3, compared against the analytical solution. Note that the soil was saturated in the middle layer. Moreover, the T-O solution produced sharp change of profiles at the interface of silty clay loam and fine sand at about 4 m depth. Overall, the solution from T-O method agreed well with the analytical solution. At the upper domain of both fine sand soils (0–1 m and 4–5 m depth), the solutions from the T-O method agreed with the analytical solution better than did Hydrus-1D.

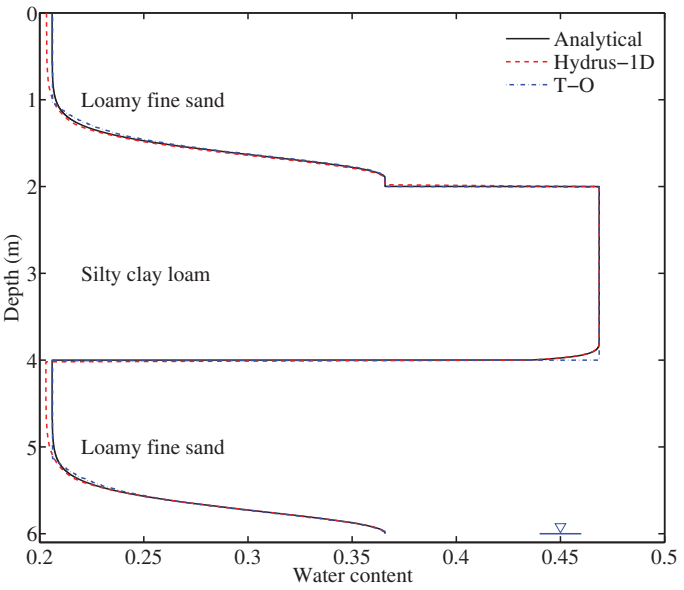

Figure 3. Steady infiltration into three-layer soil after *Rockhold et al.* [1997].

4.2. Five-Layer Infiltration Test

We tested the finite water-content methodology using results from the laboratory study of *Ma et al.* [2010] who performed a laboratory column experiment on infiltration into a 3.0 m thick soil consisting of five layers. The infiltration experiment was carried out in a transparent acrylic tube with 0.28 m inner diameter. During the experiment, a constant depth of 7.5 cm ponding was maintained, and the cumulative infiltration and infiltration rate were measured. The properties of the soil layers are listed in Table 2. Figure 4 shows the temporal evolution of the water content profiles as simulated by the finite water-content methodology and Hydrus 1-D. Figure 5 shows the infiltration rate and cumulative infiltration over time for this test for both tested models.

Table 2. Soil Layer Properties for Five-Layer Infiltration Test [after *Ma et al.*, 2010]

Soil Depth (m)	Texture	K_s (cm h^{-1})	α (cm^{-1})	n	θ_r	θ_s	θ_i
0.0–1.0	Silt loam	0.8778	0.0111	1.2968	0.06	0.50	0.16
1.0–1.2	Loam	1.1544	0.0105	1.5465	0.08	0.51	0.14
1.2–1.5	Silt loam	0.7536	0.0069	1.5035	0.12	0.46	0.16
1.5–1.8	Loam	0.3030	0.0086	1.6109	0.14	0.50	0.19
1.8–3.0	Silt loam	0.7980	0.0054	1.5090	0.08	0.49	0.13

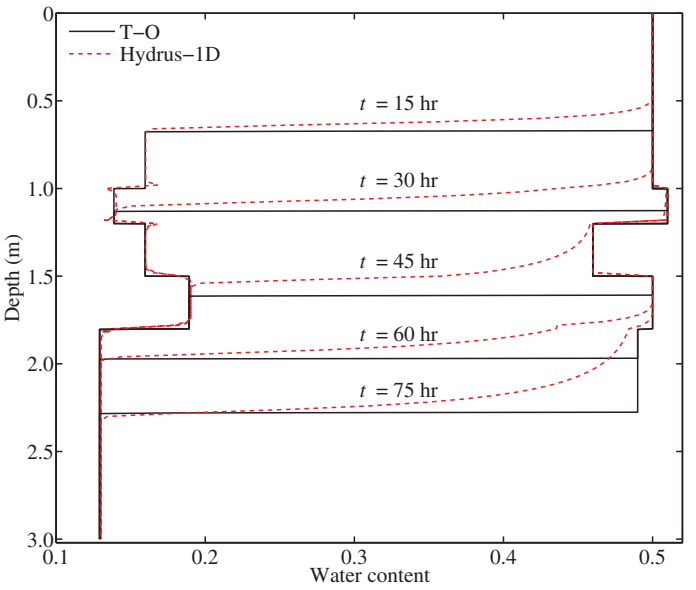

Figure 4. Water content profile evolution during five-layer infiltration test after *Ma et al.* [2010].

As seen in Figure 4, sharp wetting fronts were observed in T-O method compared to the smooth profiles predicted by Hydrus-1D. *Ma et al.* [2010] reported that Hydrus-1D artificially smoothed the wetting front compared to the observations. The simulated infiltration rate and cumulative infiltration agreed well with measurements. At time around 50 h, there was a decrease in infiltration rate simulated by both the T-O method and Hydrus-1D that agreed with observations as the wetting front reached layer 4, where the hydraulic conductivity was much smaller than other layers. The simulated depth of wetting fronts from both the T-O method and Hydrus-1D lagged behind the measured depth. This was caused by the effect of trapped air that reduced the effective porosity and caused the actual depth of the infiltration front to exceed that modeled by both approaches [*Ma et al.*, 2010].

4.3. Eight Month Test with Loam Soil, Shallow Groundwater, and Evapotranspiration

In this test we used 8 months of 15 min rainfall data collected in central Panama between 6 May and 31 December 2009, which corresponds to the wet season. The total rainfall for this period was 2630 mm, and the potential annual evapotranspiration (ET) was approximately 540 mm as calculated from meteorological station data using the Priestley-Taylor method with coefficient calibrated by *Ogden et al.* [2013].

The test was patterned after a riparian area. The soil was assumed a homogeneous layer of loam 1.0 m thick, with a static water table 1.0 m below the land surface. Soil parameters assumed in the test included: effective porosity θ_e =0.43, residual saturation: θ_r =0.027, saturated hydraulic conductivity K_s=1.04 cm h^{-1}, and van Genuchten parameters n = 1.56 and α = 0.036 cm^{-1}. The root zone was assumed to be 0.5 m thick, and the wilting point was −15 bar. Actual ET was assumed equal to potential ET when the root zone maximum water content was greater than the assumed field capacity water content θ_{fc}=0.32, and decreased linearly between the field capacity and wilting point water content θ_{wp}=0.03.

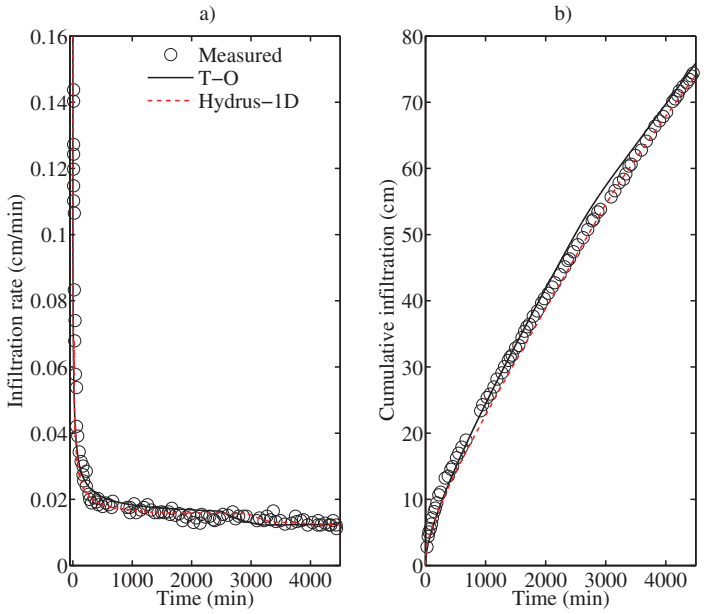

Figure 5. Infiltration rate comparison between Hydrus 1-D and finite water-content infiltration method for five-layer infiltration test [*Ma et al.* 2010].

Cumulative infiltration, runoff, groundwater recharge, and evapotranspiration are shown in Figure 6. Performance

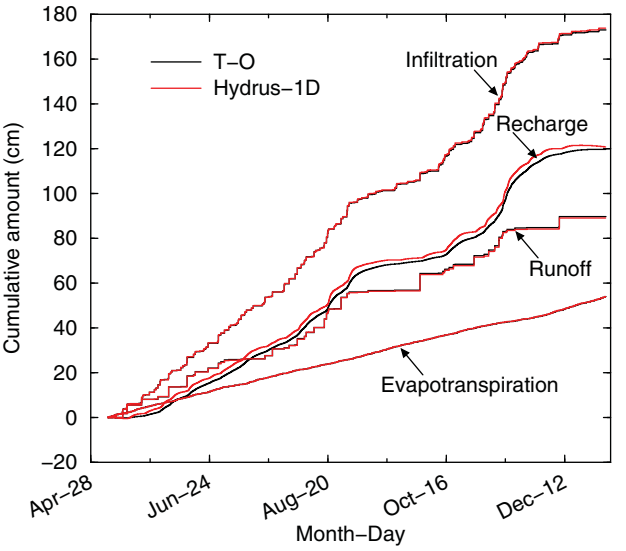

Figure 6. Cumulative fluxes from 8-month simulation test using rainfall and ET data from Panama, and identical soil properties and van Genuchten parameters to estimate $\psi(\theta)$ and $K(\theta)$ for Loam soil.

metrics are listed in Table 3. Note that in terms of fluxes, the Nash-Sutcliffe efficiency (NSE) comparing the finite water-content discretization against the Hydrus-1D solution is >0.99. The percent bias (PBIAS) was calculated as:

$$PBIAS = \left[\frac{\sum_{i=1}^{n}\left(Y_o^i - Y_s^i\right)}{\sum_{i=1}^{n} Y_o^i}\right] * 100 \text{ percent}, \quad (24)$$

where Y_o is the observed (Hydrus-1D) flux value and Y_s is the simulated (T-O) value, all at time i.

The cumulative fluxes shown in Figure 6 are very similar for both Hydrus-1D and T-O. The soil water profiles during the simulation are different for the finite water-content approach and for the numerical solution of Richards' equation. Figure 7 shows water content profiles at $t=50$, 100, 150, and 200 days into the simulation for Hydrus 1-D and the finite water-content solutions. Notice the jagged nature of the finite water-content profiles, compared to the smoother Hydrus 1-D profiles. It is noteworthy that with the differences in these profile snapshots, the infiltration flux calculated by these two methods is almost identical.

Differences in the infiltration, runoff, recharge, and evapotranspiration fluxes are plotted in Figure 8 for the 8 month simulation period. Differences (cm) were calculated as T-O minus Hydrus-1D. The largest difference is in the amount of recharge, where the T-O method took approximately 2.5 cm of water from the groundwater up into the vadose zone during the first approximately 30 days of the simulation. From that point on, there was slightly less recharge because the T-O method predicted about 0.7 cm (0.8%) more runoff and about 0.7 cm less infiltration than Hydrus-1D. Compared to the 263 cm total amount of rainfall, these 0.7 cm differences in infiltration and runoff are quite inconsequential, amounting to about 0.27 percent of the total rainfall.

Table 3. Performance of the Finite Water-Content Solution Compared Against Hydrus-1D for the 8 Month Test on a Loam Soil With Evapotranspiration

Cumulative Flux	NSE (-)	PBIAS (%)	RMSE (cm)	T-O (cm)	Hydrus-1D (cm)	Difference (cm)
Infiltration	0.9999	0.34	0.4	173.1	173.8	−0.7
Recharge	0.9961	3.91	2.5	119.7	120.8	−1.1
Runoff	0.9998	−0.63	0.4	89.7	89.0	0.7
ET	1.0	0.13	0.0	54.0	54.1	−0.1

4.4. Eight Month Test With Shallow Groundwater on 12 Soil Textures Without Evapotranspiration

We ran the finite water-content algorithm on 12 USDA soil textures using the default van Genuchten parameters from Hydrus-1D [*Simunek et al.* 2005] listed in Table 4, and compared the T-O results against Hydrus-1D simulations using the same parameter values. These simulations used the same eight month Panama rainfall data set without evapotranspiration. ET was not included because differences between the way the Hydrus-1D and the T-O method take ET from the profile has a significant effect in soil textures that are finer than the loam soil shown in Figure 6. In the T-O method, ET is taken from the right-most bin(s) in the root zone, whereas in Hydrus-1D water is taken using a spatial root distribution function, independent from water content except that removal of soil water stops when the wilting point is reached. This creates significantly different soil water profiles that cause large differences in infiltration and runoff in the case of some of the finer soil textures. Root water uptake occurs preferentially from the wetter zones of the soil

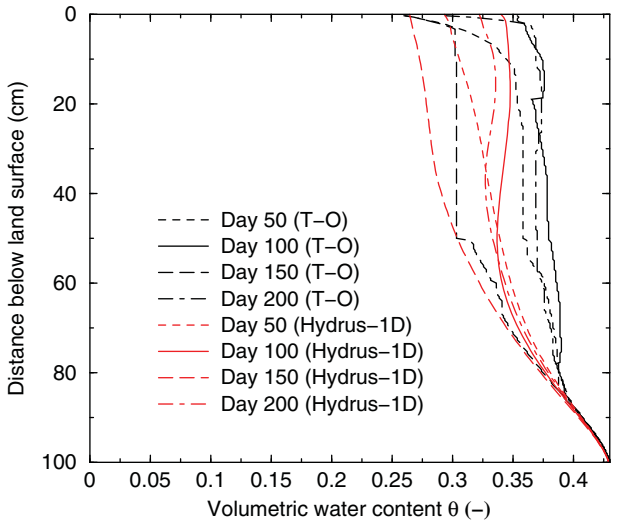

Figure 7. Water content profiles during 8-month simulation at four different times during the 8-month simulation test on a Loam soil with evapotranspiration.

from both empirical and theoretical evidence [*Green and Clothier*, 1995], which indicates that the T-O approach is perhaps more valid. However, this difference prevents meaningful comparison with ET.

Simulation results on the 12 USDA soil textures and no evapotranspiration are listed in Table 5. In general, these results show that the agreement between Hydrus 1D and T-O is best for the nine coarsest soils. The three finest soil textures would not converge in Hydrus-1D unless we set the air entry pressure to a value of −2 cm, which has a significant effect on the hydraulic conductivity function. This change in air entry pressure was not necessary in the T-O method, and makes comparison of the two methods for those soils meaningless. Therefore, we limit our discussion of results to the nine coarsest soils in Table 5.

In terms of infiltration, the Nash-Sutcliffe Efficiencies (NSEs) are greater than or equal to 0.88 for the coarsest nine soils. The groundwater recharge NSEs are greater than 0.92 for the nine coarsest soils, while the surface runoff NSEs are greater than or equal to 0.88 for all soils except sandy loam, which produced little runoff. Note in Table 5 that the column labeled "Diff. H-1D" shows the difference in cumulative flux defined as T-O minus Hydrus-1D (cm) divided by the total cumulative flux from Hydrus-1D, expressed as a percentage. Similarly, the column labeled "Diff. Total" is the difference between T-O and Hydrus-1D divided by the amount of total rainfall in the test, 263 cm, expressed as a percentage. Compared to Hydrus-1D, the T-O method tended to overpredict infiltration in soils three through nine. The percentage differences of the T-O method versus Hydrus-1D in terms of the Hydrus-1D cumulative infiltration vary from 0 to 16.7 percent. When normalized by total rainfall, the differences in cumulative infiltration vary from 0 percent to 5.7 percent in these tests without ET.

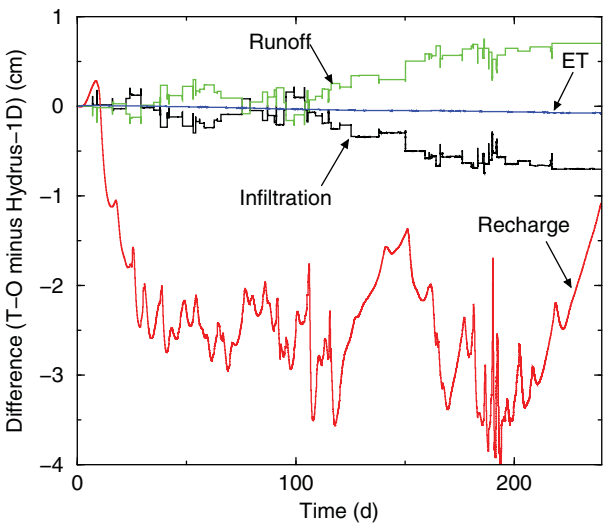

Figure 8. Differences in runoff, infiltration, evapotranspiration, and recharge amounts over the 8 month infiltration test with 263 cm total rainfall for a loam soil.

4.5. Computational Efficiency

Whereas Hydrus-1D has been continually improved since before 1991, our method combining equations (18), (19), and (21), was first run in December 2014. At present, our run times are comparable to Hydrus-1D. We believe that in time our method will prove to be considerably less computational expensive than the numerical solution of the *Richards* [1931] equation. The fact that our method is arithmetic and an explicit ODE solution suggests that it will be amenable to significant improvements in computational efficiency.

5. Discussion

The finite water-content method is more intuitive in some ways than the numerical solution of the Richards PDE, trading

Table 4. Soil Properties and van Genuchten Parameters Tested in 8 Month Test With Shallow Water Table and Without Evapotranspiration

Soil	θ_r	θ_e	α (cm^{-1})	n	K_s (cm h^{-1})
Sand	0.045	0.43	0.145	2.68	29.70
Loamy sand	0.057	0.41	0.124	2.28	14.59
Sandy loam	0.065	0.41	0.075	1.89	4.42
Loam	0.078	0.43	0.036	1.56	1.04
Silt	0.034	0.46	0.016	1.37	0.25
Silt loam	0.067	0.45	0.02	1.41	0.45
Sandy clay loam	0.1	0.39	0.059	1.48	1.31
Clay loam	0.095	0.41	0.019	1.31	0.26
Silty clay loam	0.089	0.43	0.01	1.23	0.07
Sandy clay	0.1	0.38	0.027	1.23	0.12
Silty clay	0.07	0.36	0.005	1.09	0.02
Clay	0.068	0.38	0.008	1.09	0.2

numerical complexity for accounting complexity, because keeping track of fronts in bins requires elegant coding. As opposed to the numerical solution of equations (1), (2), or (3), which represent an advection/diffusion solution that perhaps overemphasizes the importance of soil water diffusivity [*Germann*, 2010], our method neglects soil water diffusivity and is therefore advection-dominant, which makes it tend to preserve sharp fronts owing to the fact that flow preferentially advances through the larger θ portion of the profile, and is pulled to the left to higher ψ portions of the profile by the zero-dimensional process of capillary relaxation. Results of the three-layer steady infiltration test and five-layer unsteady infiltration test show that compared to an analytical solution and laboratory data, the finite water-content method is in some ways superior than the numerical solution of equation (3). This is particularly true in terms of matching observed sharp infiltration fronts, while agreeing with calculated flux in the unsteady case.

The differences in water content profiles shown in Figure 7 for the 8 month test are striking. Yet the similarity of the fluxes calculated by the two methods indicates the nonunique nature of the problem and the correctness of the finite water-content approach. The excellent agreement shown in Figure 6 supports the hypothesis that the improved T-O method is an ODE alternative approximation to the *Richards* [1931] PDE. Those results, together with those from *Ogden et al.* [2015b], suggest that the cross partial-derivative term that arose in the derivation (equation (10)) is negligible in the finite water-content discretization.

As shown in Table 5, 8 month simulations without ET on the 12 soil textures with van Genuchten parameters listed in Table 4 demonstrate runoff NSEs greater than 0.87 in predicting infiltration on the nine

Table 5. Results of Vadose Zone Simulation Tests on 12 USDA Soil Classifications Using 8 Month Panama Rainfall, With Total Rainfall 263 cm, Groundwater Table Fixed at 1 m Below Land-Surface, and No Evapotranspiration[a]

	Cumulative Infiltration						Cumulative Recharge						Cumulative Runoff					
Soil No., Texture	NSE	T-O (cm)	H-1D (cm)	Diff. (cm)	Diff. H-1D (%)	Diff. Total (%)	NSE	T-O (cm)	H-1D (cm)	Diff (cm)	Diff. H-1D (%)	Diff. Total (%)	NSE	T-O (cm)	H-1D (cm)	Diff. (cm)	Diff. H-1D (%)	Diff. Total (%)
1. Sand	1.00	262.8	262.8	0.0	0.0	0.0	1.00	258.9	260.4	−1.4	−0.6	−0.6	-	0.0	0.0	0.0	0.0	0.0
2. Loamy sand	1.00	262.8	262.8	0.0	0.0	0.0	1.00	258.4	260.2	−1.8	−0.7	−0.7	-	0.0	0.0	0.0	0.0	0.0
3. Sandy loam	1.00	254.6	246.9	7.7	3.1	2.9	1.00	250.4	244.8	5.6	2.3	2.1	−0.21	8.2	15.9	−7.6	−48.2	−2.9
4. Loam	0.97	185.9	171.6	14.3	8.3	5.4	0.98	182.9	170.2	12.7	7.4	4.8	0.90	76.9	91.2	−14.3	−15.6	−5.4
5. Silt	0.96	102.3	93.5	8.8	9.5	3.4	0.98	100.0	92.3	7.6	8.3	2.9	0.99	160.5	169.3	−8.9	−5.2	−3.4
6. Silt loam	0.96	134.0	121.7	12.3	10.1	4.7	0.97	131.9	120.7	11.3	9.3	4.3	0.97	128.8	141.1	−12.3	−8.7	−4.7
7. Sandy clay loam	0.96	184.1	169.0	15.1	8.9	5.7	0.98	180.1	166.9	13.3	8.0	5.0	0.88	78.7	93.9	−15.2	−16.2	−5.8
8. Clay loam	0.93	91.9	81.4	10.5	12.9	4.0	0.95	89.9	80.4	9.5	11.8	3.6	0.99	170.9	181.4	−10.6	−5.8	−4.0
9. Silty clay loam	0.88	40.8	34.9	5.8	16.7	2.2	0.92	39.1	34.1	5.1	14.9	1.9	1.00	222.0	227.9	−5.9	−2.6	−2.2
*10. Sandy clay	0.69	51.4	71.7	−20.4	−28.4	−7.8	0.59	48.0	70.7	−22.7	−32.1	−8.6	0.96	211.4	191.1	20.4	10.7	7.7
*11. Silty clay	0.47	12.7	20.2	−7.5	−37.0	−2.8	0.42	12.3	20.1	−7.8	−38.8	−3.0	1.00	250.1	242.6	7.5	3.1	2.8
*12. Clay	0.80	60.5	77.9	−17.5	−22.3	−6.6	0.83	60.0	74.9	−14.9	−20.0	−5.7	0.97	202.3	184.9	17.3	9.4	6.6

[a]Notes: H–1D=Hydrus-1D. *Denotes soils where Hydrus-1D would converge only if the air entry pressure was set to −2 cm.

coarsest soils. The three finest soils are excluded from comparison because Hydrus-1D failed to converge on those soils unless we set the air entry pressure to be −2 cm, a physically unrealistic value for those soils. The T-O method had no convergence difficulties on those soils. When the numerical solution of Richards' equation does not converge, time is wasted and the solver must give up and at best revert to some approximate solution. Our solution method does not suffer from this problem, and is therefore more reliable. Because our solution is a set of ODEs, we anticipate some very efficient numerical solvers will be developed for our method.

In terms of water balance, differences between infiltration calculated using Hydrus-1D and the T-O method ranged from 2.2 to 5.7 percent of rainfall over the 8 month period on the nine coarsest soils in simulations without ET (Table 5). In terms of infiltration and runoff, NSE values were greater than or equal to 0.88 in all soils except sandy loam, which produced very little runoff. These NSE values indicate that the improved T-O method has considerable skill compared to the numerical solution of *Richards'* [1931] equation in predicting hydrologic fluxes in the vadose zone and runoff generation.

While it is not necessary to attribute actual pore-sizes to the finite water-content bins, this could be done. This would allow simulation of high Bond number bins that are associated with non-Darcian fluxes such as film or gravity driven preferential flows [*Or*, 2008]. Examples of these are flows through macropores or cracks. These techniques remain to be developed.

6. Conclusions

We used a hodograph transformation, finite water-content discretization, and the method of lines to produce a set of three ordinary differential equations to calculate one-dimensional vertical flow in an unsaturated porous medium. Comparisons with the numerical solution of *Richards'* [1931] equation (RE) using Hydrus-1D and data from laboratory tests support the hypothesis that the finite water-content method first published by *Talbot and Ogden* [2008] and modified as described in this paper is an alternative to the RE solution for an unsaturated, incompressible soil that is homogeneous in layers. Our continuous method is an entirely new class of approximate solution that has considerable predictive skill compared to the numerical solution of RE with and without a shallow water table.

The method was derived from conservation of mass in an unsaturated porous medium and unsaturated Buckingham-Darcy law. Our finite volume solution is guaranteed to conserve mass, is explicitly integrable using analytical or numerical ODE solvers and therefore has no convergence limitations. The finite water-content formulation avoids the problems associated with the numerical solution of the PDE form of Richards' equation near saturation [*Vogel et al.*, 2001] and when sharp fronts occur. The finite water-content approach is general in that any monotonic form of the empirical water retention and conductivity relations may be used and the method will remain stable.

The derivation assumed that the soil is homogeneous and incompressible within layers and neglected the nonwetting phase. Vertically variable soil properties require identification of soil layers that are each uniform in properties. Soil layers in our solution communicate with each other through a head boundary condition, and require a matched flux across layer boundaries.

The results indicate that the derived ODE method and its three forms that model infiltration, falling slugs, and groundwater fronts is a viable alternative to the numerical solution of *Richards'* [1931] PDE in homogeneous soil layers for the simulation of infiltration. That the method is guaranteed to conserve mass, is explicit and therefore has no convergence limitations, and is numerically simple suggest its use in critical applications such as high-resolution quasi-3D simulations of large watersheds or in regional coupled models of climate and hydrology where hundreds of thousands to millions of instances of a vadose zone solver are required.

Acknowlegments:
Contribution: Improvements to the *Talbot and Ogden* [2008] algorithm were collaboratively made by Fred Ogden, Wencong Lai, and Bob Steinke, with the addition of capillary relaxation, falling slugs, and groundwater table dynamic effects on the vadose zone. Fred Ogden performed the original derivation of the T-O equation presented herein. Bob Steinke added falling slugs to the simulation code using a linked-list methodology. Julian Zhu served as an internal reviewer. Cary Talbot participated in discussions and provided the improved finite water-content figures. John Wilson suggested that the improved T-O method might be closer to RE than we had originally supposed, improved, and verified the derivation. This work was funded by the U.S. National Science Foundation, EPSCoR program through cooperative agreement 1135483 Collaborative Research: CI-WATER, Cyberinfrastructure to Advance High Performance Water Resource Modeling. Dani Or was instrumental in discussing the physical aspects of water behavior in the vadose zone. Craig C. Douglas and Vitaly Zlotnik provided useful input on the computer science and mathematics of our solution. Nels Frazier discovered that capillary relaxation of infiltration or groundwater fronts is equivalent to a numerical sort. Glenn Warner reviewed an earlier draft of this paper. We acknowledge the constructive review comments of WRR editor Graham Sander, Philip Broadbridge, and one anonymous reviewer. Panama rainfall data were provided by NSF EAR-1360384 WSC-Category 2 Collaborative Research: Planning and Land Management in a Tropical Ecosystem: Complexities of Land-use and Hydrology Coupling in the Panama Canal Watershed, and the Smithsonian Tropical Research Institute. Data / model statement: The code and data used for the 8 month infiltration test is available from http://dx.doi.org/10.15786/M2WC70. A video of the 8 month infiltration simulation on loam soil, with infiltration using Panama rainfall and ET data using the finite water-content discretization is available on you tube: http://youtu.be/vYwixGnTgms

References

Arya, L. M., and J. F. Paris (1981), A physicoempirical model to predict the soil moisture characteristic from particle size distribution and bulk density data, *Soil Sci. Soc. Am. J.*, *45*, 1023–1030.

Barry, D. A., J. Y. Parlange, R. Haverkamp, and P. J. Ross (1995), Infiltration under ponded conditions: 4. An explicit predictive infiltration formula, *Soil Sci.*, *160*(1), 8–17.

Basha, H. A. (2000), Multidimensional quasi-linear steady infiltration toward a shallow water table, *Water Resour. Res.*, *36*(7), 1697–1705.

Celia, M. A., E. T. Bouloutas, and R. L. Zarbo (1990), A general mass-conservative numerical solution for the unsaturated flow equation, *Water Resour. Res.*, *26*(7), 1483–1496.
Chen, Z., R. S. Govindaraju, and M. L. Kavvas (1994), Spatial averaging of unsaturated flow equations under infiltration conditions over areally heterogeneous fields: 1. Development of models, *Water Resour. Res.*, *30*(2), 523–533.
Childs, E. C., and A. Poulovassilis (1962), The moisture profile above a moving water table, *J. Soil Sci.*, *13*(2), 271–285.
Charbeneau, J., and R. G. Asgian, (1991), Simulation of the transient soil water content profile for a homogeneous bare soil, *Water Resour. Res.*, *27*(6), 1271–1279.
Clapp, R. B., G. M. Hornberger, and B. J. Cosby (1983), Estimating spatial variability in soil moisture with a simplified dynamic model, *Water Resour. Res.*, *19*(3), 739–745.
Corradini, C., F. Melone, and R. E. Smith (1997), A unified model for infiltration and redistribution during complex rainfall patterns, *J. Hydrol.*, *192*(1), 104–124.
Dagan, G., and E. Bresler (1983), Unsaturated flow in spatially variable fields: 1. Derivation of models of infiltration and redistribution, *Water Resour. Res.*, *19*(2), 413–420.
Downer, C. W., and F. L. Ogden (2003), Prediction of runoff and soil moistures at the watershed scale: Effects of model complexity and parameter assignment, *Water Resour. Res.*, *39*(3), 1045, doi:10.1029/2002WR001439.
Downer, C. W., and F. L. Ogden (2004), GSSHA: Model to simulate diverse stream flow producing processes, *J. Hydrol. Eng.*, *9*(3), 161–174.
Duke, H. R. (1972), Capillary properties of soils-Influence upon specific yield, *Trans. ASAE*, *688–691*.
Fatichi, S., V. Y. Ivanov, and E. Caporali (2012), A mechanistic ecohydrological model to investigate complex interactions in cold and warm water-controlled environments: 1. Theoretical framework and plot-scale analysis, *J. Adv. Model. Earth Syst.*, *4*, M05002, doi:10.1029/2011MS000086.
Gardner, W. R., D. Hillel, and Y. Benyamini (1970), Post-irrigation movement of soil water: 1. Redistribution, *Water Resour. Res.*, *6*(3), 851–861.
Germann, P. (2010), Comment on ''Theory for source-responsive and free-surface film modeling of unsaturated flow'', *Vadose Zone J.*, *9*(4), 1000–1101.
Gilding, B. H. (1991), Qualitative mathematical analysis of the Richards Equation, *Transp. Porous Media*, *5*, 651–666.
Gray, W. G., and S. Hassanizadeh (1991), Paradoxes and realities in unsaturated flow theory, *Water Resour. Res.*, *27*(8), 1847–1854.
Grayson, R. B., I. D. Moore, and T. A. McMahon (1992), Physically based hydrologic modeling: 1. A terrain-based model for investigative purposes, *Water Resour. Res.*, *28*(10), 2639–2658.
Green, W. H., and G. A. Ampt (1911), Studies on soil physics, 1, The flow of air and water through soils, *J. Agric. Sci.*, *4*(1), 1–24.
Green, S. R., and B. E. Clothier (1995), Root water uptake by kiwifruit vines following partial wetting of the root zone, *Plant Soil*, *173*(2), 317–328.
Hamdi, S., W. E. Schiesser, and G. W. Griffiths (2007), Method of lines, *Scholarpedia*, *2*(7), 2859, doi:10.4249/scholarpedia.2859, last accessed Dec. 23, 2014.
Haverkamp, R., and J.-Y. Parlange (1986), Predicting the water-retention curve from a particle-size distribution: 1. Sandy soils without organic matter, *Soil Sci.*, *142*(6), 325–339.
Haverkamp, R., J.-Y. Parlange, J. L. Starr, G. Schmitz, and C. Fuentes (1990), Infiltration under ponded conditions: 3. A predictive equation based on physical parameters, *Soil Sci.*, *149*(5), 292–300.
Hilpert, M. (2010), Explicit analytical solutions for liquid infiltration into capillary tubes: Dynamic and constant contact angle, *J. Colloid Interface Sci.*, *344*, 198–208.
Loague, K. M., and R. A. Freeze (1985), A comparison of rainfall-runoff modeling techniques on small upland catchments, *Water Resour. Res.*, *21*(2), 229–248.
Kibler, D. F., and D. A. Woolhiser (1972), Mathematical properties of the kinematic cascade, *J. Hydrol.*, *15*(2), 131–147.
Kirkland M. R., R. G. Hills, and P. J. Wierenga (1992), Algorithms for solving Richards' equation for variably saturated soils, *Water Resour. Res.*, *28*(8), 2049–2058.
Lai, W., F. L. Ogden, R. C. Steinke, and C. A. Talbot (2015), An efficient and guaranteed stable numerical method for continuous modeling of infiltration and redistribution with a shallow dynamic water table, *Water Resour. Res.*, *51*, 1514–1528, doi:10.1002/2014WR016487.
Lee, H. S., C. J. Matthews, R. D. Braddock, G. C. Sander, and F. Gandola (2004), A MATLAB method of lines template for transport equations, *Environ. Model. Software*, *19*, 603–614, doi:10.1016/j.envsoft.2003.08.017.
Liskovets, O. A (1965), The method of lines, *Differ. Equ.*, *1*(12), 1308–1323.
Ma, Y., S. Feng, D. Su, G. Gao, and Z. Huo (2010), Modeling water infiltration in a large layered soil column with a modified Green–Ampt model and HYDRUS-1D, *Comput. Electron. Agric.*, *71*, S40–S47.
Milly, P. C. D. (1986), An event-based simulation model of moisture and energy fluxes at a bare soil surface, *Water Resour. Res.*, *22*(12), 1680–1692.
Moebius, F., D. Canone, and D. Or (2012), Characteristics of acoustic emissions induced by fluid front displacement in porous media, *Water Resour. Res.*, *48*, W11507, doi:10.1029/2012WR012525.
Morel-Seytoux, H. J., F. N. Correia, J. H. Hyre, and L. A. Lindell (1984), Some recent developments in physically based rainfall-runoff modeling, in *Frontiers in Hydrology*, edited by W. H. C. Maxwell and L. R. Beard, pp. 37–51, Water Resour. Publ., Littleton, Colo.
Morel-Seytoux, H. J., P. D. Meyer, M. Nachabe, J. Tourna, M. Th. Van Genuchten, and R. J. Lenhard (1996), Parameter equivalence for the Brooks-Corey and van Genuchten soil characteristics: Preserving the effective capillary drive, *Water Resour. Res.*, *32*(5), 1251–1258.
Morrow, N. R., and C. C. Harris (1965), Capillary equilibrium in porous materials, *Soc. Petrol. Eng. J.*, *5*(1), 15–24.
Nachabe, M. H. (2002), Analytical expressions for transient specific yield and shallow water table drainage, *Water Resour. Res.*, *38*(10), 1193, doi:10.1029/2001WR001071.
Niedzialek, J. M, and F. L. Ogden (2004), Numerical investigation of saturated source area behavior at the small catchment scale, *Adv. Water Resour.*, *27*(9), 925–936.
Niswonger, R. G., and D. E. Prudic (2004), Modeling variably saturated flow using kinematic waves in MODFLOW, in *Groundwater Recharge in a Desert Environment: The Southwestern United States*, edited by J. F. Hogan, F. M. Phillips, and B. R. Scanlon, pp. 101–112, AGU, Washington, D. C.
Ogden, F. L., and B. Saghafian (1997), Green and Ampt infiltration with redistribution, *J. Irrig. Drain. Eng.*, *123*(5), 386–393.
Ogden, F. L., T. D. Crouch, R. F. Stallard, and J. S. Hall (2013), Effect of land cover and use on dry season river runoff, runoff efficiency, and peak storm runoff in the seasonal tropics of central Panama, *Water Resour. Res.*, *49*, 8443–8462, doi:10.1002/2013WR013956.
Ogden, F. L., W. Lai, and R. C. Steinke (2015a), ADHydro: Quasi-3D high performance hydrological model, in *Proceedings of SEDHYD 2015, 10th Interagency Sedimentation Conference, 5th Federal Interagency Hydrologic Modeling Conference April 19–23, Reno, Nevada, USA*. [Available at http://acwi.gov/sos/pubs/3rdJFIC/index.html (accessed 27 May 2015).]

Ogden, F. L., W. Lai, R. C. Steinke, and J. Zhu (2015b), Validation of finite water-content vadose zone dynamics method using column experiments with a moving water table and applied surface flux, *Water Resour. Res.*, 10.1002/2014WR016454, in press.
Or, D. (2008), Scaling of capillary, gravity and viscous forces affecting flow morphology in unsaturated porous media, *Adv. Water Resour.*, *31*, 1129–1136, doi:10.1016/j.advwatres.2007.10.004.
Or, D., P. Lehmann, E. Shahraeeni, and N. Shokri (2013), Advances in soil evaporation physics: A review, *Vadose Zone J.*, *12*(4), 1–16, doi: 10.2136/vzj2012.0163.
Parlange J.-Y., I. Lisle, R. D. Braddock, and R. E. Smith (1982), The three parameter infiltration equation, *Soil Sci.*, *133*(6), 337–341.
Parlange, J.-Y., R. Haverkamp, and J. Touma (1985), Infiltration under ponded conditions: 1. Optimal analytical solution and comparison with experimental observation, *Soil Sci.*, *139*(4), 305–311.
Parlange, J.-Y., D. A. Barry, M. B. Parlange, W. L. Hogarth, R. Haverkamp, P. J. Ross, L. Ling, and T. S. Steenhuis (1997), New approximate analytical technique to solve Richards equation for arbitrary surface boundary conditions, *Water Resour. Res.*, *33*(4), 903–906.
Philip, J. R. (1957), The theory of infiltration: 1. The infiltration equation and its solution, *Soil Sci.*, *83*(5), 345–357.
Richards, L. A. (1931), Capillary conduction of liquids in porous mediums, *J. Appl. Phys.*, *1*(5), 318–333.
Rockhold, M. L., C. S. Simmons, and M. J. Fayer (1997), An analytical solution technique for one-dimensional, steady vertical water flow in layered soils, *Water Resour. Res.*, *33*(4), 897–902.
Ross, P. J. (1990), Efficient numerical methods for infiltration using Richards' equation, *Water Resour. Res.*, *26*(2), 279–290.
Salvucci, G. D., and D. Entekhabi (1995), Ponded infiltration into soils bounded by a water table, *Water Resour. Res.*, *31*(11), 2751–2759.
Simunek, J., M. Th. van Genuchten, and M. Sejna (2005), The HYDRUS-1D software package for simulating the movement of water, heat, and multiple solutes in variably saturated media, version 3.0, HYDRUS software series 1, Dep. of Environ. Sci., Univ. of Calif. Riverside, Riverside, Calif.
Smith, R. E. (1983), Approximate soil water movement by kinematic characteristics, *Soil Sci. Soc. Am. J.*, *47*(1), 3–8.
Smith, R. E., and R. H. B. Hebbert (1983), Mathematical Simulation of Interdependent surface and subsurface hydrologic process, *Water Resour. Res.*, *19*(4), 987–1001.
Smith, R. E., and J.-Y. Parlange (1978), A parameter-efficient hydrologic infiltration model, *Water Resour. Res.*, *14*(3), 533–538.
Smith, R. E., C. Corradini, and F. Melone (1993), Modeling infiltration for multistorm runoff events, *Water Resour. Res.*, *29*(1), 133–144.
Talbot, C. A., and F. L. Ogden (2008), A method for computing infiltration and redistribution in a discretized moisture content domain, *Water Resour. Res.*, *44*, W08453, doi:10.1029/2008WR006815.
Talsma T., and J.-Y. Parlange (1972), One-dimensional vertical infiltration, *Aust. J. Soil Res.*, *10*(2), 143–150.
Tocci, M. D., C. T. Kelley, and C. T. Miller (1997), Accurate and economical solution of the pressure-head form of Richards' equation by the method of lines, *Adv. Water Resour.*, *20*(1), 1–14.
Triadis D., and P. Broadbridge (2012), The Green-Ampt limit with reference to infiltration coefficients, *Water Resour Res.*, *48*, W07515, doi: 10.1029/2011WR011747.
van Dam, J. C., and R. A. Feddes (2000), Numerical simulation of infiltration, evaporation, and shallow groundwater levels with the Richards' equation, *J. Hydrol.*, *233*(1–4), 72–85.
van Genuchten, M. Th. (1980), A closed-form equation for predicting the hydraulic conductivity of unsaturated soils, *Soil Sci. Soc. Am. J.*, *44*(5), 892–898.
Vogel, T., M. Th. van Genuchten, and M. Cislerova, (2001), Effect of the shape of the soil hydraulic functions near saturation on variably-saturated flow predictions, *Adv. Water Resour.*, *24*(2), 133–144.
Wilson, J. L. (1974), Dispersive mixing in a partially saturated porous medium, PhD dissertation, 355 pp., Dep. of Civ. Eng., Mass. Inst. of Technol., Cambridge, U. K.
Yu, H., C. C. Douglas, and F. L. Ogden, (2012), A new application of dynamic data driven system in the Talbot-Ogden model for groundwater infiltration, *Procedia Comput. Sci.*, *9*, 1073–1080.
Zaidel, J., and D. Russo (1992), Estimation of finite difference interblock conductivities for simulation of infiltration into initially dry soils, *Water Resour. Res.*, *28*(9), 2285–2295.